Influence of Crystallization Conditions on the Microstructure and Electromechanical Properties of Poly(vinylidene fluoride−trifluoroethylene−chlorofluoroethylene) Terpolymers

Rob J. Klein,[†] J. Runt,[‡] and Q. M. Zhang*[,‡,§]

Materials Research Institute, Department of Materials Science and Engineering, and Department of Electrical Engineering, The Pennsylvania State University, University Park, Pennsylvania 16802

Received June 3, 2003; Revised Manuscript Received July 17, 2003

ABSTRACT: The crystallization process and its influence on the microstructures and in turn the ferroelectric and electromechanical properties of poly(vinylidene fluoride−trifluoroethylene−chlorofluoroethylene) (P(VDF−TrFE−CFE)) terpolymer were investigated. It was found that, in addition to the crystallites formed at the isothermal crystallization temperature T_x, further crystallites form during the rapid cooling from T_x to room temperature. The proportion of lower melting crystallites increases with T_x, and for $T_x = 142$ °C, this proportion is more than 90%. The experimental results show that the lower melting crystallites have a higher fraction of the all-trans conformation (and thus more polar-phase component) than the crystallites formed at T_x. As a result, the higher T_x samples show an increased polarization hysteresis and reduced electric field induced strain response. For example, the strain is reduced from −5.9 to −4.2% as T_x is increased from 112 to 142 °C. In addition, the experimental results in combination with other reported results indicate that CFE units are included in the crystalline lattice. Consequently, the influence of CFE on the ferroelectric behavior of the polymer is through the defects induced in the crystal lattice.

I. Introduction

Polymers for electromechanical applications offer many unique and inherent advantages when compared with other materials, being lightweight, flexible, and relatively easy to process and form into complicated shapes or large areas.[1,2] Among various electromechanical polymers, ferroelectric poly(vinylidene fluoride) (PVDF) and its copolymer with trifluoroethylene (TrFE) exhibit the highest known piezoelectric response and have consequently found many commercial applications.[1−3] Since the discovery of high piezoelectricity in PVDF more than 30 years ago, there has been constant effort in improving the electromechanical performance of this class of polymers.[1−7]

Recently, it was demonstrated that, by appropriate high-energy electron irradiation treatment, the piezoelectric P(VDF−TrFE) copolymer can be converted into an electrostrictive polymer with an electrostrictive strain greater than 5% and elastic energy density greater than 1 J/cm^3, which are orders of magnitude larger than those of piezoelectric P(VDF−TrFE) copolymers.[8−10] This high strain and elastic energy density are due to defects induced by the irradiation, which weaken the polarization coupling and convert the P(VDF−TrFE) to a relaxor ferroelectric. Microstructural studies indicate that the electromechanical response of the high-energy electron-irradiated P(VDF−TrFE) copolymer originates from a field-induced molecular conformation change, which in the crystal lattice can generate strain of more than 10%.[1,8]

More recently, it was further demonstrated that, by copolymerizing P(VDF−TrFE) with a small amount of chlorinated monomer such as chlorofluoroethylene (CFE), one can realize the same macroscopic response as that achieved by high-energy electron irradiation.[10,11] In this paper, we will examine one of these terpolymers, P(VDF−TrFE-CFE), investigating how the ferroelectric and electromechanical responses are influenced by polymer crystallization processes in tandem with the corresponding microstructure changes.

The main objective of this paper is to investigate the effect of crystallization temperature on the microstructure and electromechanical response of the terpolymer. Through this investigation, it is also intended to examine how the termonomer CFE influences the microstructures. It was found that, by varying the crystallization temperature, one can selectively vary the fraction of polar and nonpolar crystallites in the crystalline phase. Crystallites formed during long times at the crystallization temperature T_x exhibit less polar behavior. Crystallites formed during the rapid cooling process between T_x and room temperature exhibit stronger polar behavior. This is established most quantitatively by wide-angle X-ray diffraction (WAXD) and reinforced by FT-IR, polarization loop, and electromechanical strain measurements. Furthermore, DSC results show that the fraction of crystallites formed at T_x decreases as T_x is increased from 112 to 142 °C. At $T_x = 142$ °C, DSC data indicate that more than 90% of the crystallites are formed during the rapid cooling. As will be shown, crystallizing at higher T_x has an adverse effect on the electromechanical strain response and increases the polarization loop hysteresis.

On the basis of these as well as other related results, it can also be deduced that CFE termonomers are included in the crystalline phase, creating local defect random fields and destabilizing the macropolar phase with respect to the nonpolar phase in the polymer.

II. Experimental Section

P(VDF−TrFE−CFE) at a composition of 68/32/9 mol % was chosen for this study due to its relatively high electromechani-

[†] Materials Research Institute.
[‡] Department of Materials Science and Engineering.
[§] Department of Electrical Engineering.

10.1021/ma034745b CCC: $25.00
Published on Web 08/19/2003

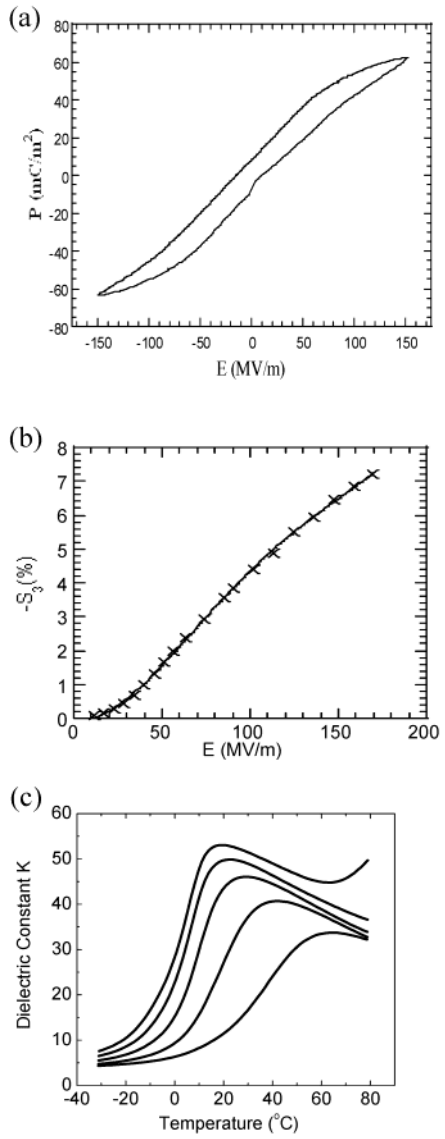

Figure 1. (a) Room temperature polarization hysteresis loop and (b) field-induced strain measured at 1 Hz (crosses are data points and solid curve is drawn to guide the eyes); (c) dielectric constant as a function of temperature at different frequencies: 0.1, 1, 10, 100, and 1000 kHz (from top to bottom). The data are for the terpolymer P(VDF−TrFE−CFE) 68/32/9 mol %.

cal response among the terpolymer compositions investigated. To facilitate the discussion and comparison with the P(VDF−TrFE) copolymer, the composition of the terpolymer is labeled as VDF_x−$TrFE_{1-x}$−CFE_y, where the mole ratio of VDF/TrFE is $x/(1 - x)$ and y is the mol % of CFE in the terpolymer. Presented in Figure 1 is a brief summary of the electrical and electromechanical properties of this terpolymer. The polarization hysteresis loop measured at room temperature is shown in Figure 1a and the corresponding thickness strain in Figure 1b. An electric-field-induced strain of more than 7% can be achieved. Figure 1c shows the dielectric constant as a function of temperature measured at different frequencies. The terpolymer exhibits a relatively high room temperature dielectric constant, and the maximum of the broad dielectric peak shifts progressively toward higher temperatures, behavior typical of relaxor ferroelectrics.[12,13]

The terpolymers were synthesized via suspension polymerization using an oxygen-activated initiator.[14] The resulting terpolymer was then dissolved in DMF and cast as 20 μm films. To examine the influence of isothermal crystallization temperature on the crystallinity, structure, and resulting functional properties, the terpolymer was heated to 200 °C

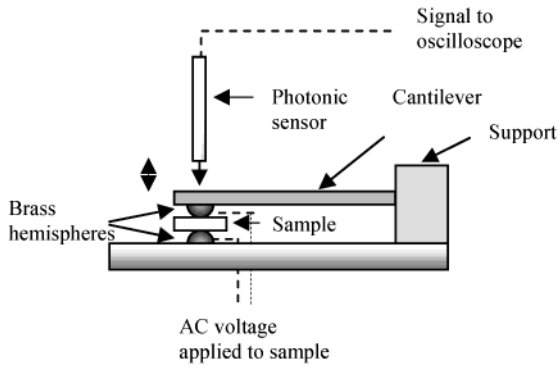

Figure 2. Schematic drawing of the thickness strain measurement setup.

($> T_m$) for ∼45 min and then cooled quickly (30 °C/min) to a predetermined crystallization temperature. Each sample was maintained at the desired crystallization temperature, T_x, for >16 h for most samples and then quickly cooled to room temperature at a rate of ∼30 °C/s. T_x examined in this study ranged from 112 to 142 °C. DSC experiments were carried out in heating at a rate of 10 °C/min (TA Instrument Q100). The conformations of the terpolymers were characterized by FT-IR spectroscopy using a Nicolet FT-IR spectrometer in the temperature range from room temperature to 160 °C. X-ray studies were carried out at the Synchrotron X-ray Light Source at Brookhaven National Laboratory, beamline X-18A. The wavelength used was 1.2399 Å. For electrical characterization, gold electrodes were sputtered on the two sample surfaces. Polarization hysteresis loops were characterized using a Sawyer−Tower circuit, and the field-induced strain was measured using a photonic sensor. In the latter setup, the polymer film was placed between two conductive hemispheres as schematically shown in Figure 2, in which one hemisphere is attached to a fixed sample holder and the other to a steel cantilever beam. Strain in the polymer film caused the head of the cantilever beam to move along the z-direction, which was monitored by a photonic sensor (MTI2000).[15]

III. Experimental Results and Discussion

3.1. Nature of the Termonomer Inclusion. As with any random copolymerization of semicrystalline polymers, there is the question as to the degree of inclusion of the copolymer units in the crystalline regions. For the case of the copolymer P(VDF−TrFE), the VDF and TrFE units are chemically quite similar (the size of hydrogen and fluorine are very close) and consequently easily cocrystallize.

Crystallization of the P(VDF−TrFE−CFE) terpolymers is more complicated, however. To begin, we treat this terpolymer as a copolymer between VDF−TrFE and CFE. Moreover, the fraction of CFE is relatively small (in our case 9%), so the bulk of the material acts as the P(VDF−TrFE) copolymer disturbed by occasional defects of CFE. Assuming random polymerization of the CFE, which is suggested from all the experimental evidence to date, there are a few possible scenarios for placement of the CFE in the crystallites: (1) total exclusion (no CFE in the crystalline phase), (2) partial inclusion, and (3) inclusion with CFE aggregation within the crystallites. Experimental evidence strongly discourages total exclusion. First of all, if we assume that the 9% termonomer is more or less equally spaced in the terpolymer chain, the distance between termonomer units ranges from ∼26 to 29 Å (depending on which conformation is used). (To allow for this statistical prediction, relatively high crystallinity and random placement of the termonomer units must exist, and both

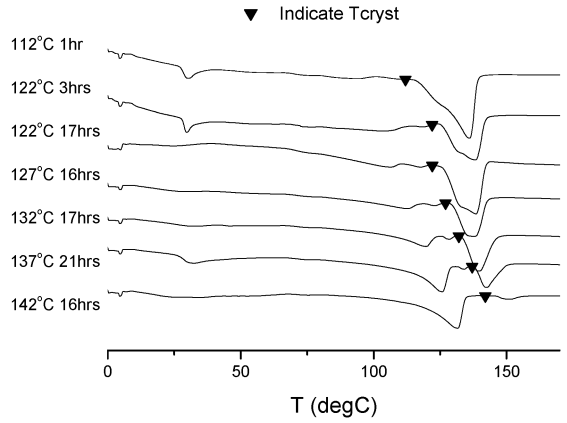

Figure 3. DSC traces of the terpolymer samples with varying isothermal crystallization temperature T_x. In the figure, both T_x and the crystallization time of each sample are indicated. The arrowhead indicates the temperature position of T_x relative to each trace.

have been observed.) If total exclusion occurs, the lamellar thickness cannot exceed this distance between termonomer units. Crystallites thinner than 30 Å will, however, melt at temperatures much less than 100 °C, which is not observed.[9,16,17] Second, the thickness of a similar terpolymer system has been shown by small-angle scattering to range from 170 to 240 Å[18] (for chlorotrifluoroethylene (CTFE) as the termonomer with CTFE concentrations of 11.5 and 4.5%). Third, analysis of the conformations and unit cell parameters of the P(VDF−TrFE−CFE) terpolymer by FT-IR and WAXD, respectively, show major deviations from the P(VDF−TrFE) copolymer. For example, a large decrease in all-trans conformation and an increase in the interchain spacing after adding CFE can be seen by comparing the terpolymer data in Figures 5 and 9, respectively, with that of the copolymer.[19] These results can be attributed to the defects introduced by the large chlorine atom in the CFE unit being included in the crystallites. Finally, computer simulations of short chains of terpolymers with CFE and other chlorinated-termonomer terpolymers indicate that inclusion of the CFE unit is a low-energy process that occurs quite naturally.[20] In fact, the simulation results have shown that in P(VDF−TrFE) copolymers in the VDF/TrFE ratio similar to the terpolymer studied here there is very small energy difference between all-trans (polar) conformation and trans−gauche (TGTG′) and T_3GT_3G' conformations.[21] All of these factors lead to the conclusion that CFE units are included in the crystalline regions.

3.2. DSC Results. Figure 3 summarizes the DSC thermograms for the terpolymer crystallized from 112 to 142 °C and then quenched to room temperature. As T_x increases, a melting peak at temperatures below T_x gradually appears. For the terpolymer samples with a T_x of 142 °C, the lower temperature melting peak is dominant, indicating that most of the crystallites were formed during the rapid cooling process. In comparison, no such behavior was ever observed for the P(VDF−TrFE) copolymers: the CFE unit significantly slows the crystallization process and is responsible for the two observed melting endotherms.[9,22] The presence of CFE monomer in the VDF−TrFE polymer chains significantly lowers the crystallinity and crystal growth rate when compared with the copolymer.[9,22] Table 1 lists values for the heats of fusion, melting temperatures, and crystallinities for the terpolymer crystallized at various

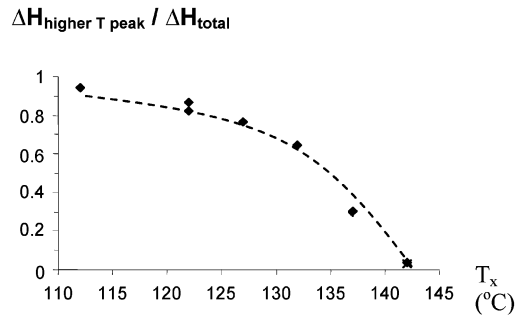

Figure 4. Ratio f_H of ΔH from the higher melting crystallite to the total heat of fusion (from both the higher and lower melting crystallites) as a function of T_x. The data show a monotonic decrease of this ratio with T_x. Data points are shown, and the dashed curve is drawn to guide the eyes.

Table 1.

polymer	T_x (°C)	cryst time (h)	ΔH (J/g)	$T_m(1)$ (°C)	$T_m(2)$ (°C)	X_C
copolymer	140	16	31		158	74
terpolymer	112	1	17		136	41
	122	3	18	103	138	44
	122	17	20	106	139	48
	127	16	20	112	138	48
	132	17	18	119	140	43
	137	21	20	126	143	47
	142	16	15	132	151	39

T_x compared against the copolymer at a similar composition (VDF/TrFE 68/32 mol %). In the table, $T_m(1)$ corresponds to the melting of the crystallites formed below T_x (i.e., during rapid cooling) and $T_m(2)$ is the melting of the crystallites formed during the long crystallization at T_x.

Interestingly, rapid cooling from the melt, or crystallization for short times at higher temperatures followed by rapid cooling, produces very low crystallinity (<20%). This may be due to rearrangement experienced by the terpolymer chains while at higher T_x, or a nucleation barrier that requires crystals formed at higher T_x over long times.

Figure 4 presents the ΔH_m of the higher temperature melting peak (normalized to the total enthalpy, which thus can be regarded as the fraction of the crystallites formed at T_x to the total crystallites at room temperature) as a function of T_x. The data reveal that as T_x increases, this ratio decreases monotonically, reflecting the increased fraction of crystallites formed during the rapid cooling process.

3.3. Wide-Angle X-ray Diffraction Data. X-ray data were collected near the $2\theta = 15°$ in order to interrogate interchain spacing and, through its peak width, crystalline order perpendicular to the chain direction. For P(VDF−TrFE) copolymers in the ferroelectric β-phase, this peak corresponds to the (110, 200) reflection.[4,22] Because of the pseudohexagonal symmetry of the crystal normal to the polymer chain direction, (110) and (200) reflections overlap and cannot be resolved. For convenience of comparison, this peak in the nonpolar hexagonal phase is still labeled as the (110, 200) reflection in the literature.[3,23,24] Here, this convention is used for the X-ray peak of the terpolymer, for which the crystal lattice should possess hexagonal symmetry perpendicular to the chain direction. Also collected was the (001) reflection, whose peak width is related to the coherent X-ray scattering domain along the polymer chain direction. For the (110, 200) reflec-

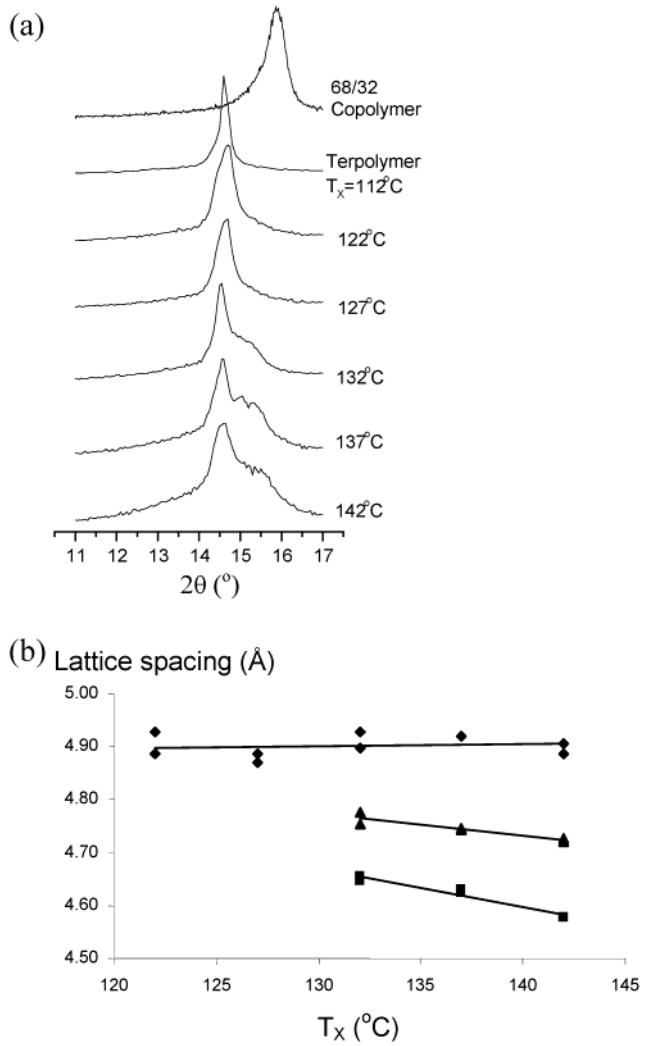

Figure 5. (a) X-ray data in the angular range of the (110, 200) reflection taken at room temperature for the terpolymers with different T_x, from which lattice constants are determined. (b) Lattice constants for the nonpolar (∼4.9 Å) and polar (triangles and squares) components of the (110, 200) reflection measured at room temperature as a function of T_x; The data for the copolymer of similar composition are also shown (from ref 13). The X-ray wavelength is 1.2399 Å.

tion, the data were acquired at selected temperatures between room temperature and T_x (taken on heating) to follow the evolution of the microstructure. For the (001) reflection, because of the limitation of the heating stage at the X-ray beamline, no measurements were taken at temperatures above 60 °C.

The X-ray data in the angle range of the (110, 200) reflection acquired at room temperature for terpolymer films with different T_x are shown in Figure 5a. For the terpolymer films with T_x at 112, 122, and 127 °C, the X-ray data are relatively well-characterized by a single peak at $2\theta = 14.7°$, which represents the nonpolar phase.[16,24] The data fitting can be improved, however, by including a small peak at 15.3°, which is close to the position of the diffraction peak expected for the polar phase of the corresponding copolymer.[16,24−26] As T_x is raised to 132 °C, this higher angle shoulder increases quite markedly, and the best fitting to the data can be achieved by including two peaks, one near 15° and the other at 15.4°. (Two higher-angle peaks are seen most clearly in the 137 °C scan.) The phenomenon of two polar peaks was examined and explained by Lovinger et al. as arising from the existence of both the planar-zigzag (all-trans) and 3/1 helical arrangements in the crystalline phase of P(VDF−TrFE) copolymers.[25,26] Figure 5b summarizes the evolution of the X-ray peak positions as T_x is raised from 112 to 142 °C. In comparison with the X-ray data of the copolymer of similar composition, it can be deduced that the peak at lower angle ($2\theta = 14.7°$) arises from the nonpolar phase while the peaks at 15° and 15.4° indicate the presence of the polar-phase component in the crystallites.

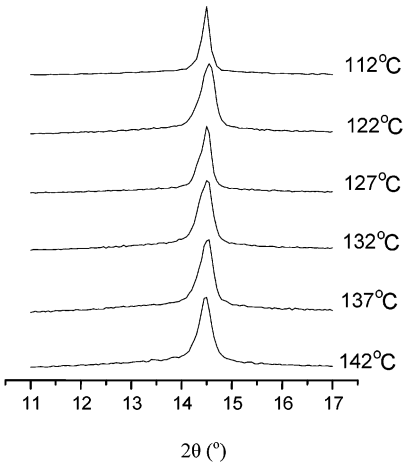

Figure 6. X-ray data for the (110, 200) reflection taken at 60 °C for the terpolymers with different T_x. The X-ray wavelength is 1.2399 Å.

Using the Scherrer equation[27]

$$L_{hkl} = \frac{0.9\lambda}{B\cos(\theta)} \tag{1}$$

the coherence of the crystal lattice perpendicular to a particular crystallographic plane can be deduced. In this equation, λ is the X-ray wavelength, B is the full width at half-maximum of the diffraction peak in question (in 2θ), and θ is the peak angular position. At room temperature, $L_{110/200} = 14$ nm for the nonpolar phase.

The X-ray data for the (110, 200) reflection acquired at 60 °C are shown in Figure 6 for terpolymer samples crystallized at different T_x. At this temperature, the shoulder corresponding to the polar phase has disappeared. Furthermore, at this temperature, the (110, 200) peaks for the samples crystallized at different T_x are nearly identical in terms of both peak position and width. Although the peak position associated with diffraction from (110, 200) of the nonpolar phase does not show much change with temperature, the peak width is reduced (to below $B(2\theta) = 0.3°$) from that at room temperature, yielding $L_{110/200} = 23$ nm at 60 °C. One explanation for the observed increase in $L_{110/200}$ is that at room temperature the nonpolar and polar phases coexist in the same crystallite, limiting the special coherence of the nonpolar phase.

It can be further deduced that in the same crystallite there are regions with higher CFE fraction, which stabilize the nonpolar phase, and regions with lower CFE, which favor the polar phase. The samples crystallized at higher T_x have a greater fraction of crystalline regions with lower CFE content (more exclusion of CFE from the crystallites) as reflected by the X-ray data. Such regions of relatively high and low CFE content are also suggested by FT-IR data.

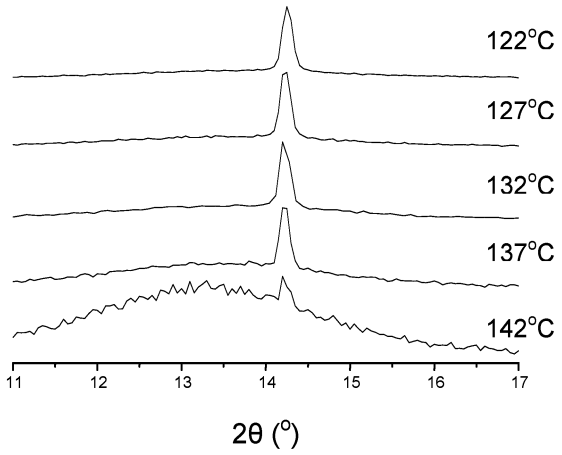

Figure 7. X-ray data for the (110, 200) reflection taken at T_x (indicated for each scan) for the terpolymer samples with different T_x. The X-ray wavelength is 1.2399 Å.

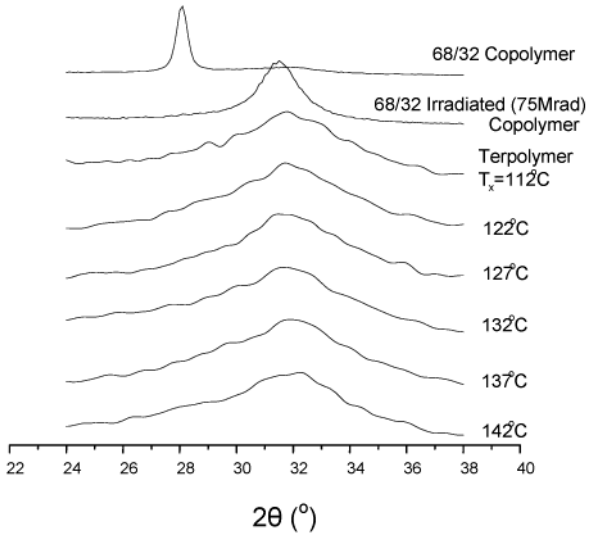

Figure 8. X-ray data in the angular range of the (001) reflection taken at room temperature as a function of T_x. For comparison, the data of copolymer and irradiated copolymer (75 Mrad) of similar composition are also shown (from ref 13). The X-ray wavelength is 1.2399 Å.

X-ray data taken at $T = T_x$ for polymer samples with different T_x are shown in Figure 7. At this temperature, the X-ray peaks arise from the diffraction of the crystallites with T_m higher than the original T_x. The (nonpolar) peak position changes only slightly with temperature due to thermal expansion. On the other hand, there is a further reduction in the breadth of the (110, 200) reflection to $B(2\theta) = 0.15°$. Therefore, the coherent domain is now larger than 42 nm.[28,29] These results indicate that $L_{110/200}$ for the crystallites formed during the rapid cooling process is at least twice as small as that formed at T_x. Furthermore, the crystallinity at the various T_x's evaluated by X-ray peak areas follows the same trend as determined by DSC, shown in Figure 4.

The (001) reflections as a function of T_x are shown in Figure 8; the peak positions are at approximately the same location as the (001) reflection of the nonpolar phase of the parent copolymer. For samples crystallized at different T_x, there is no indication of a (001) reflection from the polar phase, which is notably different than the data in the angular range of the (110, 200) reflection. This suggests very small and defective polar domains along the chain direction. The broadness of the (001) peak indicates a very small coherent size along the polymer chain direction. Using the Scherrer equation, it is deduced that the coherent X-ray scattering domain is about 1.5 nm and is the same for all samples examined. Furthermore, even when heating the polymer samples to 60 °C, at which temperature the (110, 200) reflection peak width decreases noticeably, there is no change in the (001) X-ray peak shape and width. In contrast, the copolymer shows thick nonpolar domains, with $L_{001} = 15$ nm for the 68/32 copolymer.[13] Thus, the presence of the chlorinated commoners induces nanodomains—in the stem direction, but not in the lateral direction.

Table 2.

freq (cm^{-1})	assignment	conformation	references
1290	$\nu_a(CF_2)$, $\nu_a(CC)$, $\delta(CCC)$	T_m, $m > 4$	30, 31
850	$\nu_a(CF_2)$	T_m, $m > 3$	30, 31
612	$\delta(CF_2)$, $\delta(CCC)$	TG	30, 32
510	$\delta(CF_2)$	T_3G	19, 32

3.4. FT-IR Results. In Figure 9d, the FT-IR data for the terpolymer samples with T_x at 112 and 142 °C are presented, which illustrate the change of the molecular conformations of the terpolymer samples with T_x (the copolymer is included for comparison). The absorbance peaks at 510 cm^{-1} (T_3G), 612 cm^{-1} (TG), and 1290 cm^{-1} ($T_{m>4}$) are chosen for analysis since they all represent motions of the CF_2 group to some extent.[19,30−32] In Table 2, the assignment of the vibration modes for these absorbance peaks is summarized. Because some of the peaks have relatively low intensity, direct analysis of the peak areas using a curve deconvolution routine results in relatively large error. Instead, subtraction of the data with a reference was used for data analysis. The scan taken at 155 °C (polymer melt) was used as the baseline for the 1288 and 614 cm^{-1} peaks, and the scan taken at 15 °C was used for the baseline for the 510 cm^{-1} absorbance peak. Subtraction and comparison of the peak heights at the chosen wavelengths allow qualitative analysis of the conformation changes with both temperature and crystallization temperature. Parts a, b, and c of Figure 9 give the conformation fractions for the 510 cm^{-1} (T_3G), 612 cm^{-1} (TG), and 1290 cm^{-1} ($T_{m>4}$) peaks, respectively.

Consistent with the X-ray data, at room temperature, the samples with $T_x = 142$ °C show a higher fraction of the all-trans conformation. As the temperature is raised to 50 °C, there is a drop in the all-trans conformation. The results indicate that there is a broad transition at temperatures near 40 °C, representative of a weak Curie transition. This transition temperature seems to be the same for all the samples with T_x ranging from 112 to 142 °C, although the transition is much weaker for samples with lower T_x, presumably due to the lower fraction of the polar regions in the polymers. The correlation between the size of the polar phase transition and the polymer composition again suggests that there are regions with higher CFE content (less polar) and regions with lower CFE content (more polar).

3.5. Polarization Hysteresis Loop and Electric-Field-Induced Strain Data. The polarization hysteresis loops for the terpolymer samples crystallized at different T_x are shown in Figure 10. A salient feature revealed by the data is the change of the polarization hysteresis for the terpolymer samples with different T_x. The terpolymer samples with lower T_x exhibit lower

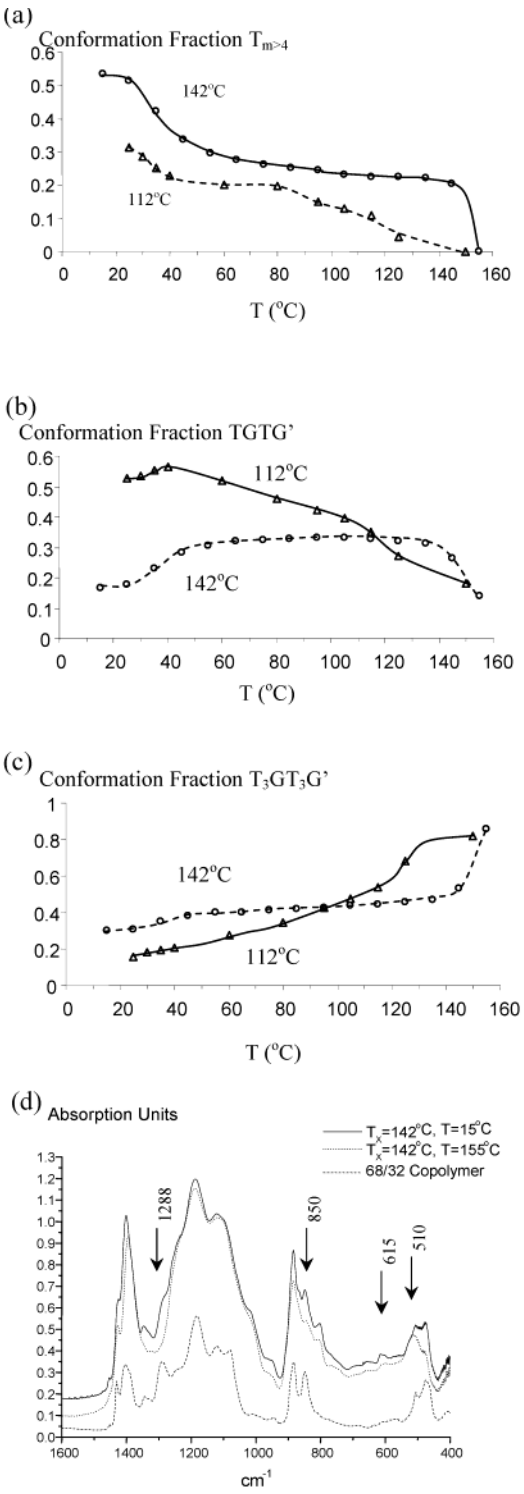

Figure 9. Comparison of the fractions of different conformations: (a) all-trans, (b) TGTG′, and (c) T_3GT_3G' as a function of temperature for the terpolymer samples with $T_x = 112$ °C (triangles) and 142 °C (open circles). (d) FT-IR scans measured at 15 and 155 °C for the terpolymer sample with $T_x = 142$ °C. The copolymer of similar composition, measured at room temperature, is also shown for reference.[29]

polarization hysteresis, i.e., a smaller P_r (remnant polarization) and E_c (coercive field). For example, the terpolymer films with $T_x = 142$ °C show an E_c of 20 MV/m, while for the sample with $T_x = 112$ °C, $E_c = 11$ MV/m.

Corresponding to this change in the ferroelectric behavior, the field-induced strain is also dependent on

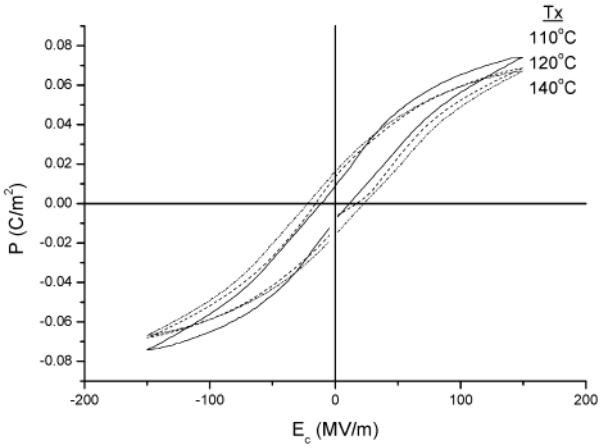

Figure 10. Polarization hysteresis loops measured at room temperature and 1 Hz for the terpolymer samples with T_x of 110, 120, and 140 °C.

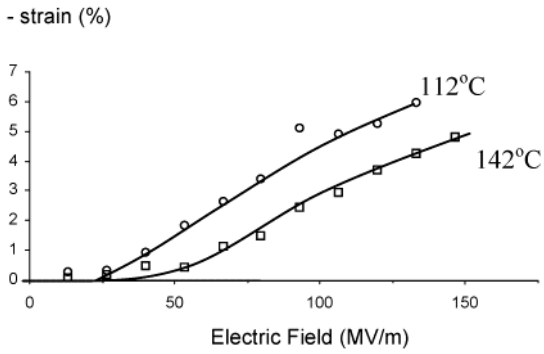

Figure 11. Thickness strain of the terpolymer as a function of the applied field for the terpolymer samples with $T_x = 112$ and 142 °C. The data were acquired at room temperature and 1 Hz ac field.

the T_x of the terpolymer samples. As shown in Figure 11, the terpolymer sample with T_x at 112 °C exhibits a field-induced strain of −5.9% at 133 MV/m, while for the samples with T_x at 142 °C, the strain is reduced to −4.2% under the same field. This is too large of a change to be accounted for by crystallinity changes alone. The lower field-induced strain is due to already-existing ferroelectric domains that do not undergo the local conformation change upon application of the electric field.

IV. Discussion and Conclusion

In this paper, we investigated (i) the crystallization process, (ii) the influence of the crystallization process on the microstructures, and (iii) the influence of the crystallization process on the ferroelectric and electromechanical responses of the P(VDF−TrFE−CFE) 68/32/9 mol % terpolymer. It was found that CFE units in the polymer chains reduce the crystallinity and crystal growth rate relative to the copolymer. As a consequence, there is in many cases significant crystal growth during rapid cooling below the isothermal crystallization temperature T_x. As T_x increases to 142 °C, very few crystallites are formed at T_x and more than 90% of the crystallites are formed in the rapid cooling process.

For the terpolymers studied here, one of the key questions is how the CFE monomers influence the ferroelectric behavior of the polymer. Without CFE, the P(VDF−TrFE) copolymer of 68/32 mol % is a normal ferroelectric, which at room temperature exhibits large

polarization hysteresis.[1] The copolymerization of CFE with VDF−TrFE markedly affects the ferroelectric behavior in the original VDF−TrFE crystal lattices. If the bulkier CFE monomers (the van der Waals radius of Cl is 0.18 nm, F is 0.13 nm, and H is 0.12 nm) are included in the crystallites, it will cause local lattice distortion and favor the formation of TG and T_3G conformations in the surrounding lattices rather than the all-trans conformation which is more closely packed. The CFE lattice defects will also reduce the crystal lattice positional ordering and decrease the melting temperature of the crystal lattice. Disorder caused by defects in the PVDF polymer has been shown to reduce ferroelectric properties in many instances.[33,34]

The experimental results presented favor the interpretation that CFE monomers, to some degree, are included in the crystalline region. Furthermore, the experimental data show that the crystallites formed during rapid cooling exhibit a higher fraction of the all-trans conformation and stronger polar ordering, while these crystallites have lower crystal lamellar thickness in comparison with the crystallites formed at T_x. This supports the idea that there is more inclusion in the crystallites formed during isothermal crystallization and less inclusion in the crystallites formed during rapid quenching.

Corresponding to the change of the crystallization process in the terpolymer with different T_x, it was observed that polarization hysteresis measured at room temperature increases and strain response decreases with T_x, reflecting an increased polar phase component in the crystalline region, due to the increased proportion of the crystallites formed during the rapid cooling from T_x.

Furthermore, this polar-phase component exhibits a broad transition in the temperature range from 30 to 50 °C, which is far below the Curie transition temperature in the parent copolymer phase, as indicated by the disappearance of the X-ray peak corresponding to the polar phase and marked reduction in fraction of the all-trans conformation from the temperature evolution of the FT-IR spectra. The temperature range of this broad transition is independent of T_x, suggesting the existence of a thermodynamically stable nanopolar phase in this terpolymer.

Acknowledgment. The authors thank Dr. F. Bauer for the synthesis of the terpolymer used in this work and the following persons for assistance in the lab and the thought process: Ma Yanyun, Dr. Wang, Xia Feng, Dae Yong Jeong, and Hengfeng Li. The financial support of this work by ONR under Grant N000140210418 is greatly appreciated. Research was carried out in part at the National Synchrotron Light Source, Brookhaven National Laboratory, which is supported by the U.S. Department of Energy, Division of Material Sciences and Division of Chemical Sciences, under Contract DE-AC02-98CH10886.

References and Notes

(1) *Electroactive Polymer (EAP) Actuators as Artificial Muscles*; Bar Cohen, Y., Ed.; SPIE: Bellingham, WA, 2001.
(2) Wang, T. T.; Herbert, J. M. In *The Application of the Ferroelectric Polymers*; Glass, A. M., Ed.; Blackie, Chapman & Hall: New York, 1988.
(3) *Ferroelectric Polymers*; Nalwa, H., Ed.; Marcel Dekker: New York, 1995.
(4) Lovinger, A. J. *Science* **1983**, *220*, 1115.
(5) Omote, K.; Ohigashi, H.; Koga, K. *J. Appl. Phys.* **1997**, *81*, 2760.
(6) Nakamura, K.; Nagai, M.; Kanamoto, T.; Takahashi, Y.; Furukawa, T. *J. Polym. Sci., Part B: Polym. Phys.* **2001**, *39*, 1371.
(7) Green, J.; Farmer, B.; Rabolt, J. *J. Appl. Phys.* **1986**, *60*, 2690.
(8) Zhang, Q. M.; Bharti, V.; Zhao, X. *Science* **1998**, *280*, 2101.
(9) Xia, F.; Wang, Y. K.; Li, H.; Huang, C.; Ma, Y.; Zhang, Q. M.; Cheng, Z.-Y.; Bateman, F. B. *J. Polym. Sci., Part A: Polym. Phys.* **2003**, *41*, 797.
(10) Zhang, Q. M.; Xia, F.; Cheng, Z.-Y.; Xu, H.; Li, H.; Poh, M.; Huang, C. *Proc. 11th Int. Symp. Electrets* **2002**, *181*.
(11) Xia, F.; Cheng, Z.-Y.; Xu, H.; Zhang, Q. M.; Kavarnos, G.; Ting, R.; Abdul-Sedat, G.; Belfield, K. D. *Adv. Mater.* **2002**, *14*, 1574.
(12) Bobnar, V.; Vodopivec, B.; Levstik, A.; Cheng, Z.-Y.; Zhang, Q. M. *Phys. Rev.* **2003**, *B67*, 94205.
(13) Cheng, Z.-Y.; Zhang, Q. M.; Bateman, F. B. *J. Appl. Phys.* **2002**, *92*, 6749.
(14) Bauer, F.; Foousson, E.; Zhang, Q. M.; Lee, L. M. *Proc. 11th Int. Symp. Electrets* **2002**, 355.
(15) Su, J.; Moses, P.; Zhang, Q. M. *Rev. Sci. Instrum.* **1998**, *69*, 2480.
(16) Sanchez, I. C.; Eby, R. K. *Macromolecules* **1975**, *8*, 638.
(17) Helfand, E.; Lauritzen, J., Jr. *Macromolecules* **1973**, *6*, 631.
(18) Balizer, E., 2003 US Navy Workshop on Acoustic Transduction Materials and Devices (May 2003, State College, PA).
(19) Xu, H.; Shanthi, G.; Bharti, V.; Zhang, Q. M. *Macromolecules* **2000**, *33*, 4125.
(20) Kavarnos, G., to be published.
(21) Cagin, T.; Su, H.; Strachan, A.; Cuitino, A.; Goddard, W. A., III. 2003 US Navy Workshop on Acoustic Transduction Materials and Devices (May 2003, State College, PA).
(22) Kodama, H.; Takahashi, Y.; Furukawa, T. *Ferroelectrics* **1997**, *203*, 433.
(23) Furukawa, T. *Phase Transitions* **1989**, *18*, 143.
(24) Baltá Calleja, F. J.; González Arche, A.; Ezquerra, T. A.; Santa Cruz, C.; Batallán, F.; Frick, B.; López Cabarcos, E. *Adv. Polym. Sci.* **1993**, *108*, 1.
(25) Lovinger, A. J.; Davis, G. T.; Furukawa, T.; Broadhurst, M. G. *Macromolecules* **1982**, *15*, 323.
(26) Lovinger, A. J.; Furukawa, T.; Davis, G.; Broadhurst, M. G. *Polymer* **1983**, *24*, 1225.
(27) Warren, B. E. *X-ray Diffraction*; Dover Publications: New York, 1990.
(28) Fernandez, M. V.; Suzuki, A.; Chiba, A. *Macromolecules* **1987**, *20*, 1806.
(29) Cheng, Z.-Y.; Olson, D.; Xu, H.; Xia, F.; Hundal, J. S.; Zhang, Q. M.; Bateman, F. B.; Kavarnos, G. J.; Ramotowski, T. *Macromolecules* **2002**, *35*, 664.
(30) Reynolds, N. M.; Kim, K. J.; Chang, C.; Hsu, S. L. *Macromolecules* **1989**, *22*, 1100.
(31) Kim, K. J.; Kim, G. B.; Valencia, C. L.; Rabolt, J. F. *J. Polym. Sci., Part B: Polym. Phys.* **1994**, *32*, 2435.
(32) Osaki, S.; Ishida, Y. *J. Polym. Sci.* **1975**, *13*, 1071.
(33) Lovinger, A. J.; Davis, D. D.; Cais, R. E.; Cais, J. M.; Kometani, J. M. *Polymer* **1987**, *28*, 617.
(34) Tashiro, K.; Kobayashi, M. *Phase Transitions* **1989**, *18*, 213.

MA034745B